Photoacoustics 42 (2025) 100689

Contents lists available at ScienceDirect

Photoacoustics

journal homepage: www.elsevier.com/locate/pacs

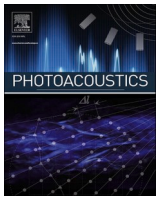

Dual-gas quartz-enhanced photoacoustic spectroscopy sensor exploiting two fiber-combined interband cascade lasers

Luigi Melchiorre [a,b], Francesco Anelli [b], Giansergio Menduni [a,*], Andrea Annunziato [b], Laurine Bodin [c], Solenn Cozic [c], Giovanni Magno [b], Angelo Sampaolo [a,d], Francesco Prudenzano [b], Vincenzo Spagnolo [a,d]

[a] PolySenSe Laboratory, Department of Physics, Polytechnic and University of Bari, Via G. Amendola 173, Bari 70125, Italy
[b] Department of Electrical and Information Engineering, Polytechnic of Bari, Via E. Orabona 4, Bari 70125, Italy
[c] Société Le Verre Fluoré, Rue Gabriel Voisin 1, Bruz 35170, France
[d] PolySenSe Innovations srl, Via G. Amendola 173, Bari 70125, Italy

ARTICLE INFO

Keywords:
QEPAS
Dual-gas sensor
IFG fiber combiner

ABSTRACT

In this work, a novel indium fluoride glass 2-input-1-output fiber combiner was designed and fabricated to combine two Interband Cascade Laser (ICL) sources emitting in the mid-infrared wavelength range. To test the combiner performance, a dual-gas quartz-enhanced photoacoustic spectroscopy sensor was demonstrated for the detection of carbon dioxide (CO_2) and nitric oxide (NO), employing two fiber-coupled ICLs having central emission wavelengths of 4,234 nm and 5,263 nm, respectively. The laser beams were coupled via the fiber combiner and then focused into a commercial acoustic detection module equipped with an input fiber-port, thus resulting in a plug-and-play sensing system. Tens of ppm-level detection limits at 3σ are achieved for both pollutants with a lock-in integration time (τ) of 0.1 s. Finally, an Allan-Werle analysis demonstrated the stability of the sensor, allowing the achievement of detection limit of 13 ppm and 4 ppm at $\tau = 10$ s for CO_2 and NO, respectively.

1. Introduction

InfraRed (IR) laser-based sensors for trace gas detection have emerged as a powerful tool in various application fields, such as environmental monitoring of polluting agents, industrial and manufacturing processes control, and diagnostic solutions for human health care [1–4]. These sensing systems leverage the unique properties of light-matter interactions to detect the presence and quantify the concentrations of specific gas molecules with high sensitivity and high selectivity [5]. Fiber-based systems play a key role in the development of innovative trace gas sensors, enabling the efficient and versatile delivery of the beam from the laser source to the sensing volume, overcoming the limitations of free-space systems [6–9]. The main advantages of implementing fibers in optical sensing include: (i) manageability – fibers are flexible and can be positioned in compact and complex arrangements, allowing for the integration of optical sensors in a wide range of environments [10]; (ii) efficiency – fibers can minimize optical losses, resulting in higher power available for sensing and thus improving the signal-to-noise ratio in the detection [11]; and (iii) stability – guided propagation of light in fibers provides enhanced stability and immunity to environmental interferences, thus improving the reliability of the gas sensing apparatus [12]. A novel development in laser-based gas sensors is the coupling of Interband Cascade Lasers (ICLs) sources, operating in the mid-IR region, with optical fibers [13,14]. This spectral region, typically defined as the wavelength range from 2.5 to 25 μm [15], is particularly interesting for gas sensing due to the presence of fundamental roto-vibrational transitions of many molecules [16]. Since silica optical fibers are not suitable to guide light with low-loss in the mid-IR wavelength range, different materials have been explored as beam delivery systems for ICLs. In recent years, Indium Fluoride Glasses (IFGs) fibers proved to be an optimal solution, since they are characterized by both low Fresnel losses and wide transmission window, from visible up to approximately 5.3 μm [17,18]. Although several laser sources have already been employed with IFG fibers [19–22], the development of fiber combiners represents a further step towards the realization of multi-gas sensors, allowing the simultaneous coupling of different laser

* Corresponding author.
E-mail address: giansergio.menduni@poliba.it (G. Menduni).

https://doi.org/10.1016/j.pacs.2025.100689
Received 7 December 2024; Received in revised form 10 January 2025; Accepted 11 January 2025
Available online 13 January 2025

sources. Indeed, this could improve the capabilities and versatility of the sensing system, enabling the integration of multiple lasers onto a single sensing platform with the aim of targeting different gas species sequentially or even simultaneously [23] and, at the same time, reducing the sensing system footprint [24].

Quartz-Enhanced Photo-Acoustic Spectroscopy (QEPAS) is a highly sensitive technique that has been widely adopted for trace gas sensing [25–29]. QEPAS is an evolution of the Photo-Acoustic Spectroscopy (PAS), relying on the photoacoustic effect for the detection, *i.e.*, the generation of acoustic waves by the target gas molecules absorbing modulated laser light and relaxing energy via non-radiative processes [30–33]. While PAS exploits microphones to detect pressure waves, in QEPAS a Quartz Tuning Fork (QTF) is employed as acoustic transducer. The QTF is coupled with resonator tubes and housed within a stainless-steel chamber, composing the Acoustic Detection Module (ADM). In QEPAS sensors, the laser beam, having an emission wavelength resonant with one (or more) optical transitions of the target gas molecules, passes through the two resonator tubes aligned with one of the vibrational antinodes of the QTF, generating acoustic waves impacting the internal surfaces of the prongs. These pressure waves put the prongs in motion, generating an electric signal due to the direct piezo-electric effect of quartz [34–36]. The electric signal is directly proportional to the concentration of the target molecules that generate the pressure waves.

In this work, we present a compact and rugged dual-gas QEPAS sensor employing two fiber-coupled mid-IR ICLs combined with a novel developed IFG fiber combiner. The two selected lasers, having a central emission wavelength of 4,234 nm and 5,263 nm, allowed the detection of carbon dioxide (CO_2) and nitric oxide (NO), respectively, representing two of the most crucial molecules in the environmental pollution processes and for diagnostic solutions in human health care [37,38].

2. Dual-Gas QEPAS Sensor

Fig. 1a shows a schematic of the employed experimental setup, while Fig. 1b depicts a photo of the fabricated fiber combiner connected to the fiber port of the ADM.

Two different Interband Cascade Lasers (ICLs), emitting at 4,234 nm (ICL #1 in Fig. 1a) and 5,263 nm (ICL #2 in Fig. 1a) were exploited to target the CO_2 absorption feature located at 2,361.46 cm^{-1} and the NO absorption feature located at 1,900.08 cm^{-1}, respectively [39]. The ICL #1 (model 3858/25–19 from Nanoplus GmbH) injection current was

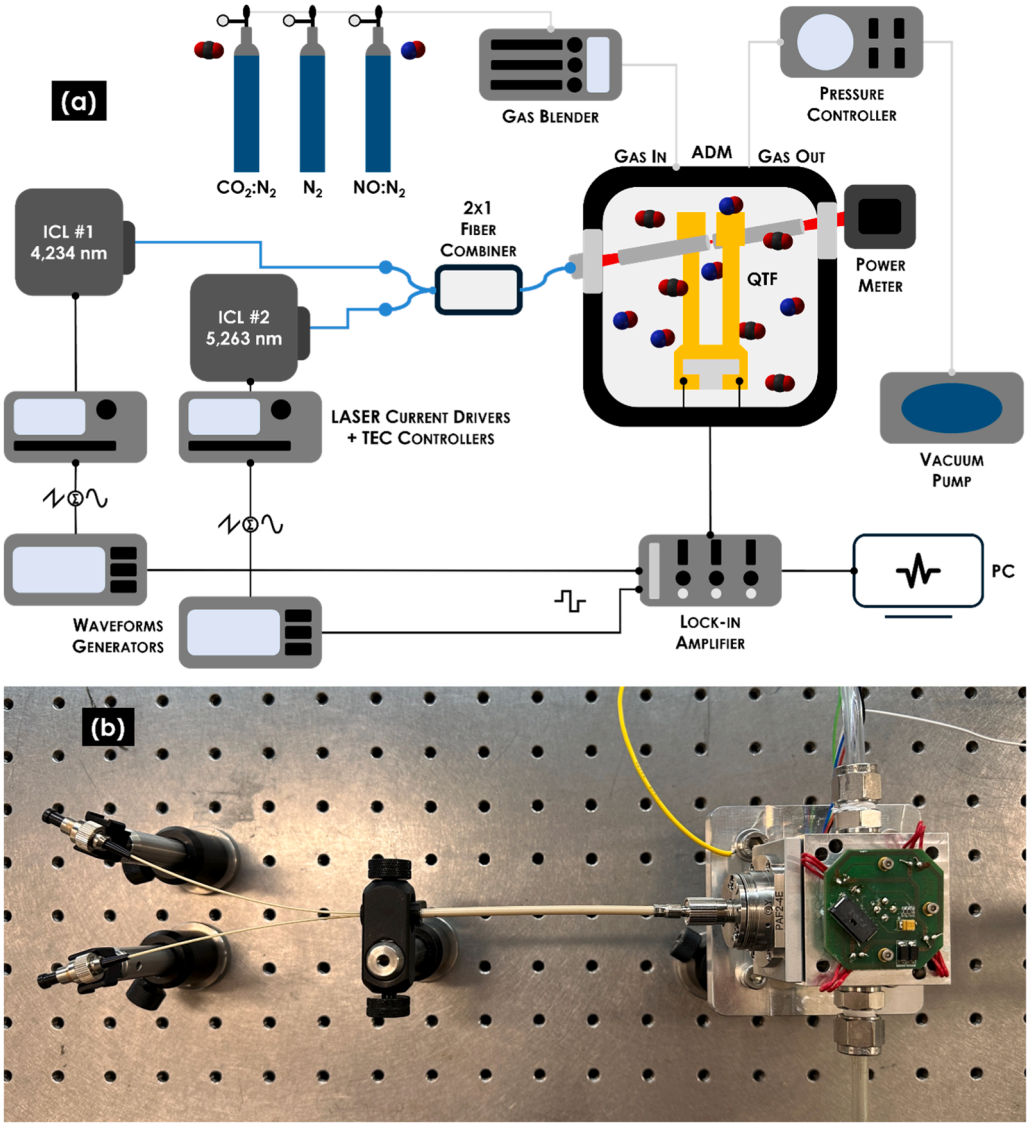

Fig. 1. (a) Schematic of the experimental setup. ICL – Interband Cascade Laser, TEC – Thermo-Electric Cooler, ADM – Acoustic Detection Module, QTF – Quartz Tuning Fork, PC – Personal Computer; (b) Photo of the custom-made 2-input-1-output fiber combiner (center-left) coupled with the ADM through its input fiber port (right).

modulated by applying a sinusoidal wave having an amplitude of 15.5 mVpp and its tuning range was scanned by superimposing a sawtooth wave having an amplitude of 50 mVpp and a frequency of 5 mHz. Likewise, the ICL #2 (model 3468/04–28 from Nanoplus GmbH) injection current was modulated by an 8 mVpp sinewave voltage added to a sawtooth wave with an amplitude of 60 mVpp and a frequency of 5 mHz. The operating temperatures of ICL #1 and ICL #2 were set to 10 °C and to 20 °C, respectively. The collimated beam of each laser was coupled into the FC/APC input connector of an Indium Fluoride Glass (IFG) fiber via a focusing lens. To mitigate etalon effects, the lens and the connector were slightly tilted and mounted into a lens tube directly UV glued (model NOA61) to the laser collimating lens (model 390036IR3, with a focal length of 4 mm and a NA of 0.56), as reported by Zifarelli *et al.* in Ref. [13]. The fabricated fiber combiner, described in the next section, allowed delivering the beam of the two fiber-coupled lasers to the fiber port (PAF2–4E from Thorlabs GmbH [40]) mounted on a commercial ADM (ADM01 from Thorlabs GmbH [41]). The fiber port, equipped with an aspheric lens having a focal length of 4 mm and an AR coating in the 2 – 5 μm range, is used to focus the light inside the ADM and between the two prongs of the QTF by passing through the resonator tubes without hitting them. Thus, the delivery of the laser beams to the input of the ADM in the reported work is fully made with optical fibers, and the beam was aligned using the five-axis translation stage of the fiber port. A mass flow-meter and pressure controller (MC3S-D from Alicat Scientific, Inc.) was employed to set and maintain a constant working pressure of the gas mixture inside the ADM, with the aid of a vacuum pump. A 3-input-channel gas mixer (GB-103 from MCQ Instruments) controlled the gas flow and enabled the generation of different gas mixtures. The developed QEPAS sensor operates at a working pressure of 300 Torr and with a total gas flow rate of 50 SCCM which resulted in the optimal working conditions. The ADM encloses the spectrophone, which consists of a T-shaped QTF acoustically coupled to a pair of metallic acoustic resonator tubes to enhance signal detection [42]. The "T" region of the QTF is 2 mm-thick and 2.4 mm-long, with prongs 1.4 mm-thick and 9.4 mm-long. Instead, the crystal width is 0.25 mm. The resonator tubes have an inner diameter of 1.6 mm and each are 12.4 mm-long [41,42]. At 300 Torr, a resonance frequency (f_r) of 12,439.55 Hz and a quality factor over 15,000 were measured. In this work, the QEPAS measurements were carried out exploiting a wavelength modulation technique along with a 2 f detection scheme: a sinewave having a frequency of $f_r/2$, generated by a waveform generator (33500B from Keysight Technologies, Inc.), was continuously applied to the ICL current driver (ITC4002QCL from Thorlabs GmbH) while the electrical signal generated by the QTF was demodulated by the lock-in amplifier (MFLI 500 kHz from Zurich Instruments Ltd.) at f_r. For all measurements, the lock-in integration time (τ) was set to 0.1 s and the sampling time was set to 3 • τ.

3. IFG Fiber Combiner

An optical fiber combiner was realized for both coupling mid-IR laser sources and QEPAS sensing with the two selected ICLs presented in the previous section. Customized IFG optical fibers with core diameter d_{co} = 25 μm and cladding diameter d_{cl} = 100 μm were fabricated by Le Verre Fluoré (Bruz, France) and their measured attenuation α is reported in Fig. 2.

The IFG optical fiber segments were cleaved with a diamond blade employing an automatic cleaver based on tension-and-scribe process. The combiner fabrication process is sketched in Fig. 3.

Firstly, as shown in Fig. 3a, the IFG optical fiber segments were inserted in a custom low-refractive index IFG tube with external diameter (d_{cap}) of 550 μm. The global structure, consisting of both optical fibers and the tube, was secured in the fiber holding blocks of the glass processing system, *i.e.*, Vytran GPX-2400, with an applied pre-tension. By means of heating and pulling technique, effectively addressing the well-known thermo-mechanical issues associated with fluoride glasses, a

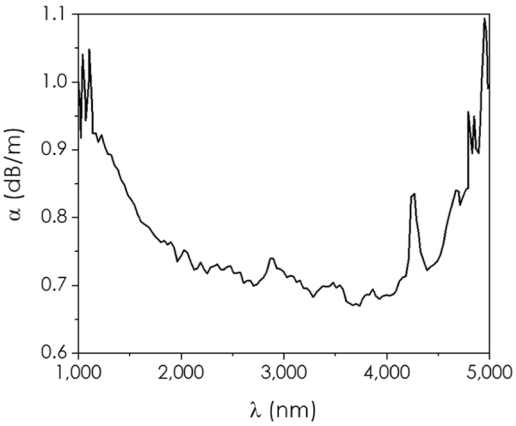

Fig. 2. Measured attenuation α, expressed in dB/m, of the IFG optical fibers employed for the combiner fabrication.

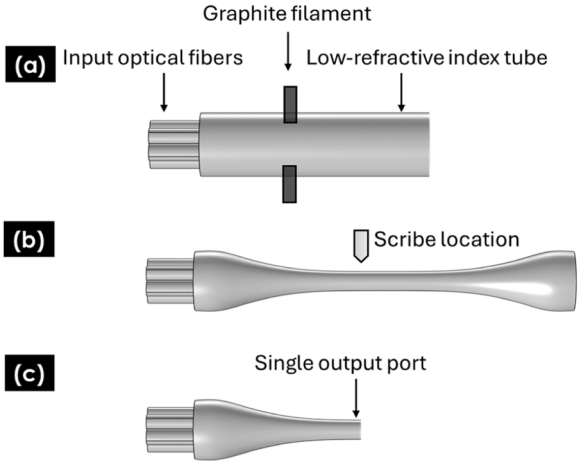

Fig. 3. Sketch of the optical fiber combiner fabrication. (a) Optical fibers inserted in a low-refractive index tube; (b) Fused bi-conical taper obtained via stretching and heating technique; (c) Cleaving of the fused bi-conical taper in the waist region.

fused bi-conical taper was obtained, as depicted in Fig. 3b [43,44]. Fig. 4 depicts a microscope image during the combiner fabrication, showing the tube containing the IFG optical fibers being drawn.

As the filament is heated, the pulling speed provided by the movement of the right fiber-holding block is greater than the feeding rate of the left fiber-holding block. This results in a reduction in diameter, as evident in Fig. 4, when comparing the non-tapered left side with the right side undergoing the drawing process. A gradual and controlled

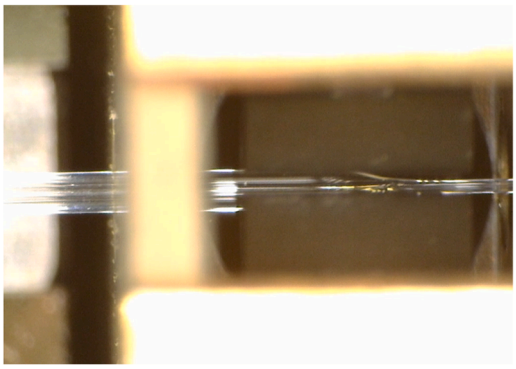

Fig. 4. Drawing of the tube containing IFG optical fibers.

down-taper transition was implemented to adhere to the adiabatic criterion, minimizing transition losses by preventing mode coupling with higher-order modes and ensuring efficient light propagation [45]. For fluoride glass processing, it is crucial to maintain stable operation during the thermal process at a temperature near the glass transition temperature (T_g) of 275 °C to prevent crystal formation [43]. This was possible by operating the commercial graphite filament of Vytran GPX-2400 with a start filament power of 12.1 W. A constant argon flow rate of 0.35 L/min inside the graphite filament is used to mitigate potential issues with air impurities or humidity. This is important, as the presence of crystallization, evident as a grainy appearance on the outer surface of the device, can lead to high insertion loss [46]. To assist the collapse of air holes and achieve a homogeneous cross-section, a pump with negative pressure was attached to one end of the tube [47]. The obtained bi-conical taper was then cleaved in the waist region, *i.e.* the narrowest point, as illustrated in Fig. 3c. This constitutes the single output port of the device. The combiner diameter in the waist region (d_w) is approximately equal to 140 μm, ensuring that the two beams at different wavelengths are spatially close, thus allowing proper alignment of the guided light at different wavelengths between the QTF prongs. The fabricated combiner was then coated and equipped with standard FC/APC connectors to (i) ensure high durability; (ii) facilitate the connection with the sources; and (iii) minimize back-reflection. The final fabricated device is reported in Fig. 1b and has a total length of 23 cm.

The measured Insertion Losses (ILs) of the fabricated 2×1 optical fiber combiner at three representative wavelengths in the mid-IR spectral range are reported in Table 1. It was verified that the device is symmetric, *i.e.*, the insertion losses do not depend on the employed input port.

These values include the coupling losses due to the connection from the ICL to the input optical fiber of the combiner and the attenuation of the employed optical fibers [18]. Both the coupling losses and the attenuation are larger at $\lambda_2 = 5{,}263$ nm than at the other tested wavelengths. These factors can partially explain the higher measured insertion loss at $\lambda_2 = 5{,}263$ nm. The device used in this work was also tested a year after its fabrication and displayed negligible signs of aging, confirming the ILs reported in Table 1.

The fabricated optical fiber combiner based on indium fluoride glass can operate at any wavelength, up to about 5,500 nm. It is worthwhile mentioning that the proposed approach is easily scalable to a higher number of input optical fibers, enabling multi-gas detection by adopting a single combiner with multiple input ports and additional lasers. An alternative solution could involve using 2×1 IFG optical fiber couplers, potentially in a cascaded configuration. For instance, the cascade of two fused couplers could merge light from three lasers emitting different wavelengths into a single common port.

For measurements requiring the combining of sources emitting at wavelengths longer than 5500 nm, other glasses, *e.g.* chalcogenide-based, could be considered. To date, the only commercially available mid-IR compatible combiners are produced by IRflex Corporation, utilizing arsenic sulfide optical fibers and supporting operation up to approximately 6,500 nm [48]. In this case, due to the high refractive index n ~ 2.4 of arsenic sulfide glass, the best theoretical transmission is only 69 % if no anti-reflection coatings are considered.

Table 1
Measured ILs of the IFG fiber combiner for three representative wavelengths.

λ (nm)	IL (dB)
3345	1.2
4234	1.1
5263	2.2

4. QEPAS Results and Discussion

The QEPAS sensor was calibrated turning sequentially ICL #1 for the detection of carbon dioxide (CO_2) and ICL #2 for the detection of nitric oxide (NO). At the output of the fiber combiner, optical power of 0.17 mW and of 0.08 mW were measured for the CO_2 and NO calibration, respectively. For both gases, QEPAS spectral scans were acquired at each concentration dilution step and representative spectra for both CO_2 and NO are shown in Fig. 5a and Fig. 5b, respectively.

No interference fringes are observed, confirming that the focused beam dimensions, achieved through the PAF2–4E fiber port lens, allowed the laser light to pass through the QTF and resonator tubes without hitting them. The tuning range of the ICL #2 allowed targeting the NO absorption features both at 1,900.08 cm^{-1} and at 1,900.52 cm^{-1} (P3 in Fig. 5b) [39]. The P1 and P2 values were retrieved and plotted as a function of the target gas concentration and the results as well as the linear best fitting curves are shown in Fig. 6.

The linear fit returned an R^2 of 0.998 and 0.9994 for the calibration of CO_2 and NO, respectively, demonstrating the linearity of the sensor. The Minimum Detection Limit (MDL) for each gas was calculated as the concentration providing a Signal-to-Noise Ratio (SNR) equal to 3. The noise level was evaluated as the standard deviation of the QEPAS signal when the emission wavelength of the laser was tuned out of any absorption feature. The sensitivities (*i.e.*, the slope of the linear fits), the noise levels, and the calculated MDLs at 3σ are reported in Table 2.

At $\tau = 0.1$ s, both MDLs are in the tens of ppm range and the realized sensor allows the monitoring of the carbon dioxide level in atmosphere [49]. Furthermore, it was experimentally verified that there are no electric interference and matrix effects between the two QEPAS signals, since no changes in the CO_2 signal, at a fixed concentration, were observed when NO traces were added in the nitrogen-based gas matrix, while the ICL #2 had been tuned far from the NO absorption features, and vice versa [50]. Finally, the Allan-Werle standard deviation analysis was employed to verify the stability of the sensor and evaluate the MDLs at different integration time [51]. For this measurement, pure nitrogen was flowing in the ADM and both lasers were tuned at an emission wavelength far from any absorption features, and the modulation was provided either to ICL #1 or to ICL #2. The results are shown in Fig. 7a and Fig. 7b.

In both cases, a similar trend was observed up to $\tau = 10$ s: the noise level slightly increases at short integration time and after a τ of 0.4 s follows a $1/\sqrt{\tau}$-like trend, as expected in a detection limited by the thermal noise of the QTF [52,53]. At τ greater than 10 s, the two curves differ. While the trend in Fig. 7b confirms a detection limited by white noise sources, mechanical instabilities in the coupling system of ICL #1 and the optical fiber cause an increase of the standard deviation. Since this difference is evident at long integration time, the developed sensor allows quasi real-time detection of both gases and the calculated MDLs at a lock-in integration time of 10 s are reported in Table 2. The CO_2 detection limits change from 31 ppm at $\tau = 0.1$ s down to 13 ppm, and from 13 ppm down to 4 ppm for the NO detection, at an integration time of 10 s.

5. Conclusions

In this work, we report on the development of a dual-gas QEPAS sensor for the detection of CO_2 and NO exploiting two fiber-coupled ICL sources combined with a novel optical fiber combiner based on IFG, whose output port was directly connected to the fiber port of an ADM. The sensor was calibrated for both gases and the linearity and the interference-free of the responses were verified. Finally, an Allan-Werle analysis was carried out to assess the stability of the sensor. Although mechanical instabilities in the ICL-fiber coupling system arising at long integration time, the developed sensor allowed CO_2 MDLs of 31 ppm at 0.1 s of integration time and of 13 ppm at $\tau = 10$ s. The NO detection is limited by the thermal noise of the sensitive element, reaching MDLs of

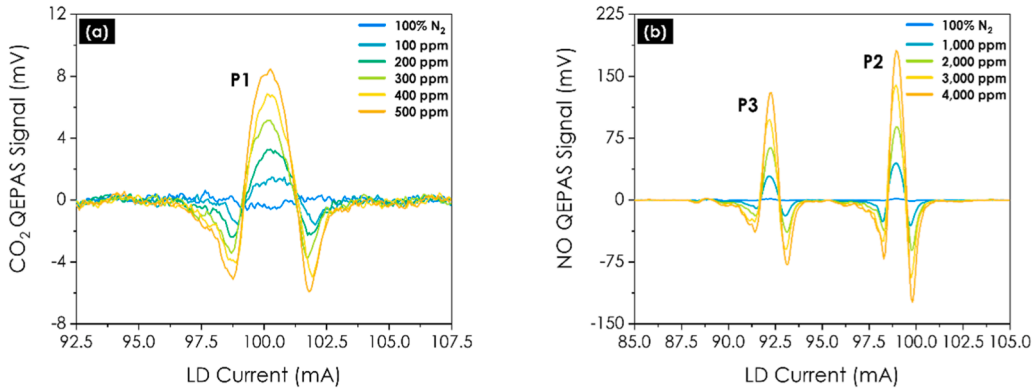

Fig. 5. Representative 2f-QEPAS spectra for (a) CO_2 concentrations from 100 ppm to 500 ppm and (b) NO concentrations from 1,000 ppm to 4,000 ppm. In both cases, the spectra measured for pure N_2 is also shown.

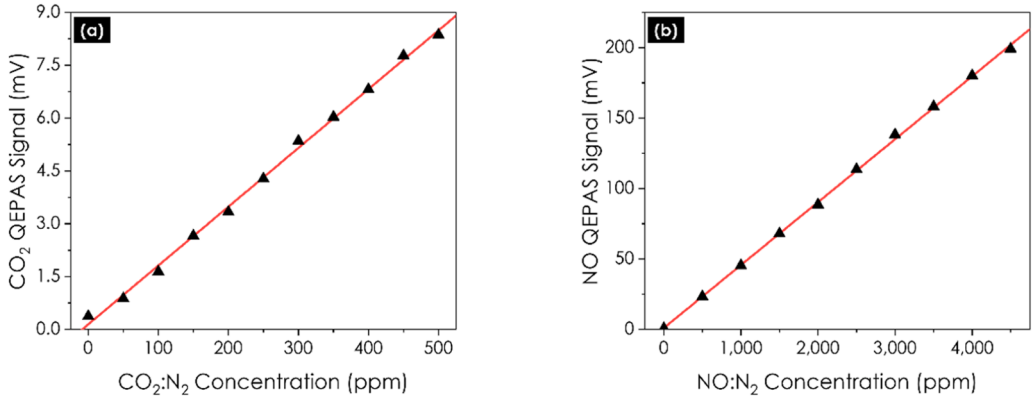

Fig. 6. QEPAS signals peak values as a function of the target gas concentration values (black triangles) and corresponding linear fit (red solid line) for (a) CO_2 and for (b) NO.

Table 2
Summary of the sensing performances of the dual-gas QEPAS sensor.

	CO_2	NO
Sensitivity	16.7 μV/ppm	44.6 μV/ppm
Noise Level	171 μV	186 μV
MDL @ 0.1 s	31 ppm	13 ppm
MDL @ 10 s	13 ppm	4 ppm

13 ppm at 0.1 s of integration time and of 4 ppm at $\tau = 10$ s. The developed dual-gas QEPAS sensor represents an innovative sensing system for the detection of multiple gases with strong absorption features in the mid-IR spectral range and proves, in addition, high sensitivity and stability, well-suited characteristics for practical, portable and field-deployable gas sensing application scenarios. The fiber coupling of mid-IR sources will be further optimized to fully exploit the optical power of lasers, thus making the proposed sensor comparable to sensing system employing free-space light sources in terms of MDL.

Author contributions

Luigi Melchiorre and Francesco Anelli equally contributed to this work.

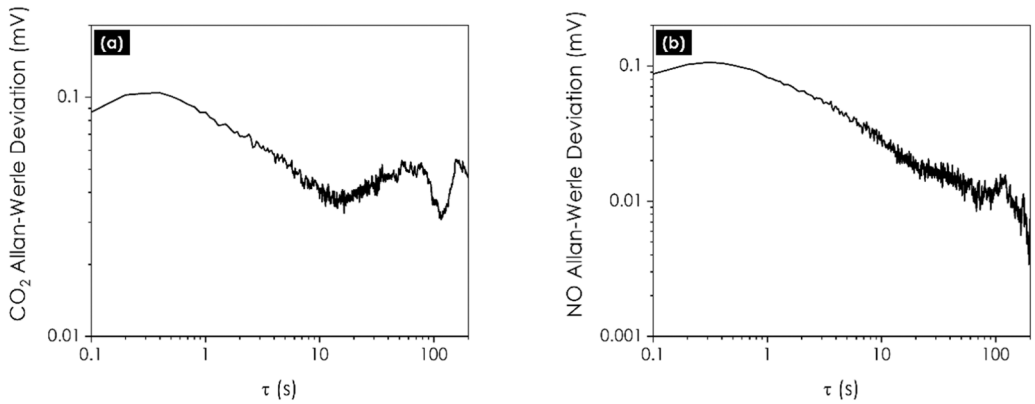

Fig. 7. Results of the Allan-Werle standard deviation analysis for the detection of (a) CO_2 with ICL #1 and (b) NO with ICL #2.

Funding

All authors acknowledge funding from the European Union's Horizon 2020 research and innovation program under grant agreement No. 101,016,956 PASSEPARTOUT, in the context of the Photonics Public Private Partnership.

The authors from Dipartimento Interateneo di Fisica di Bari acknowledge financial support from the European Union under the Italian National Recovery and Resilience Plan of NextGenerationEU MUR project PE0000023-NQSTI, project MUR – Dipartimenti di Eccellenza 2023–2027 – Quantum Sensing and Modelling for One-Health (QuaSiModO) and THORLABS GmbH within the PolySenSe joint research laboratory.

Francesco Anelli, Andrea Annunziato, and Francesco Prudenzano were also partially supported by MIUR PRIN 2022, NRPP – DD n. 1181 del 27–07–2023 - InnoVative tEchnoloGies for non-invasivE assessmenT of plAnt healTh conditIon to support precisiOn farmiNg "VEGETATION" (P2022ZF9P2, CUP: I53D23005710 001); HORIZON TMA MSCA Staff Exchanges, Project: 101182995 — ALTER-Q — HORIZON-MSCA-2023-SE-01; MIUR "Agriculture Green & Digital – AGREED", PNR 2015/20, n. ARS01_00254; the European Union under the Italian National Recovery and Resilience Plan (NRRP) of NextGenerationEU, with reference to the partnership on "Telecommunications of the Future" (PE00000001 - program "RESTART", CUP: D93C22000910001) - STRUCTURAL PROJECT Antennas & Devices foR mixing, dEtection And Manipulation of mmWaves.

CRediT authorship contribution statement

Angelo Sampaolo: Writing – review & editing, Supervision, Conceptualization. **Giovanni Magno:** Writing – review & editing, Supervision, Conceptualization. **Solenn Cozic:** Supervision, Formal analysis, Conceptualization. **Laurine Bodin:** Validation, Investigation. **Luigi Melchiorre:** Writing – original draft, Methodology, Investigation, Formal analysis, Data curation. **Vincenzo Spagnolo:** Writing – review & editing, Supervision, Funding acquisition, Conceptualization. **Francesco Prudenzano:** Writing – review & editing, Methodology, Funding acquisition, Conceptualization. **Andrea Annunziato:** Investigation, Conceptualization. **Giansergio Menduni:** Writing – original draft, Supervision, Formal analysis, Conceptualization. **Francesco Anelli:** Writing – original draft, Investigation, Data curation, Conceptualization.

Declaration of Competing Interest

The authors declare that they have no known competing financial interests or personal relationships that could have appeared to influence the work reported in this paper.

Data availability

Data will be made available on request.

References

[1] A. Genner, P. Martín-Mateos, H. Moser, B. Lendl, A quantum cascade laser-based multi-gas sensor for ambient air monitoring, Sensors 20 (2020) 1850, https://doi.org/10.3390/s20071850.

[2] Z. Du, S. Zhang, J. Li, N. Gao, K. Tong, Mid-infrared tunable laser-based broadband fingerprint absorption spectroscopy for trace gas sensing: a review, Appl. Sci. 9 (2019) 338, https://doi.org/10.3390/app9020338.

[3] S.M. Cristescu, S.T. Persijn, S. te Lintel Hekkert, F.J.M. Harren, Laser-based systems for trace gas detection in life sciences, Appl. Phys. B 92 (2008) 343, https://doi.org/10.1007/s00340-008-3127-y.

[4] G. Wysocki, Y. Bakhirkin, S. So, F.K. Tittel, C.J. Hill, R.Q. Yang, M.P. Fraser, Dual interband cascade laser based trace-gas sensor for environmental monitoring, Appl. Opt. 46 (2007) 8202, https://doi.org/10.1364/AO.46.008202.

[5] H. Moser, W. Pölz, J.P. Waclawek, J. Ofner, B. Lendl, Implementation of a quantum cascade laser-based gas sensor prototype for sub-ppmv H2S measurements in a petrochemical process gas stream, Anal. Bioanal. Chem. 409 (2017) 729–739, https://doi.org/10.1007/s00216-016-9923-z.

[6] S. Qiao, A. Sampaolo, P. Patimisco, V. Spagnolo, Y. Ma, Ultra-highly sensitive HCl-LITES sensor based on a low-frequency quartz tuning fork and a fiber-coupled multi-pass cell, Photoacoustics 27 (2022) 100381, https://doi.org/10.1016/j.pacs.2022.100381.

[7] A. Annunziato, F. Anelli, P.L.P. Du Teilleul, S. Cozic, S. Poulain, F. Prudenzano, Fused optical fiber combiner based on indium fluoride glass: perspectives for mid-IR applications, Opt. Express 30 (2022) 44160, https://doi.org/10.1364/OE.471090.

[8] S. Eilzer, B. Wedel, Hollow core optical fibers for industrial ultra short pulse laser beam delivery applications, Fibers 6 (2018) 80, https://doi.org/10.3390/fib6040080.

[9] A. Sampaolo, P. Patimisco, J.M. Kriesel, F.K. Tittel, G. Scamarcio, V. Spagnolo, Single mode operation with mid-IR hollow fibers in the range 51-105 μm, Opt. Express 23 (2015) 195, https://doi.org/10.1364/OE.23.000195.

[10] J.D. Shephard, A. Urich, R.M. Carter, P. Jaworski, R.R.J. Maier, W. Belardi, F. Yu, W.J. Wadsworth, J.C. Knight, D.P. Hand, Silica hollow core microstructured fibers for beam delivery in industrial and medical applications, Front Phys. 3 (2015), https://doi.org/10.3389/fphy.2015.00024.

[11] A. Kuhn, I.J. Blewett, D.P. Hand, P. French, M. Richmond, J.D.C. Jones, Optical fibre beam delivery of high-energy laser pulses: beam quality preservation and fibre end-preparation, Opt. Lasers Eng. 34 (2000) 273–288, https://doi.org/10.1016/S0143-8166(00)00082-8.

[12] D.P. Hand, Fiber optic high-quality Nd:YAG beam delivery for materials processing, Opt. Eng. 35 (1996) 502, https://doi.org/10.1117/1.600923.

[13] A. Zifarelli, R. De Palo, S. Venck, F. Joulain, S. Cozic, R. Weih, A. Sampaolo, P. Patimisco, V. Spagnolo, All-fiber-coupled mid-infrared quartz-enhanced photoacoustic sensors, Opt. Laser Technol. 176 (2024) 110926, https://doi.org/10.1016/j.optlastec.2024.110926.

[14] M. Giglio, P. Patimisco, A. Sampaolo, J.M. Kriesel, F.K. Tittel, V. Spagnolo, Low-loss and single-mode tapered hollow-core waveguides optically coupled with interband and quantum cascade lasers, Opt. Eng. 57 (2017) 1, https://doi.org/10.1117/1.OE.57.1.011004.

[15] Y. Ozaki, Infrared Spectroscopy—Mid-infrared, Near-infrared, and Far-infrared/Terahertz Spectroscopy, Anal. Sci. 37 (2021) 1193–1212, https://doi.org/10.2116/analsci.20R008.

[16] R.A. Kellner, R. Gobel, R. Goetz, B. Lendl, B. Edl-Mizaikoff, M. Tacke, A. Katzir, Recent progress on mid-IR sensing with optical fibers, in: A.V. Scheggi (Ed.), Chemical, Biochemical, and Environmental Fiber Sensors VII, SPIE, 1995, pp. 212–223, https://doi.org/10.1117/12.221734.

[17] J.-P. Yehouessi, S. Vidal, J.-Y. Carree, L. Bodin, S. Cozic, T. Berthelot, S. Poulain, L. Calvez, G. Huss, J. Boullet, 3 W Mid-IR supercontinuum extended up to 4.6 μm based on an all-PM thulium doped fiber gain-switch laser seeding an InF3 fiber, in: P.G. Schunemann, K.L. Schepler (Eds.), Nonlinear Frequency Generation and Conversion: Materials and Devices XVIII, SPIE, 2019, p. 6, https://doi.org/10.1117/12.2510026.

[18] J.-C. Gauthier, V. Fortin, J.-Y. Carrée, S. Poulain, M. Poulain, R. Vallée, M. Bernier, Mid-IR supercontinuum from 24 to 54 μm in a low-loss fluoroindate fiber, Opt. Lett. 41 (2016) 1756, https://doi.org/10.1364/OL.41.001756.

[19] F. Anelli, A. Annunziato, A.M. Loconsole, V.V. Francione, S. Cozic, S. Poulain, F. Prudenzano, Mid-infrared interferometry with non-adiabatic tapered ZBLAN optical fiber, Opt. Express 32 (2024) 18944, https://doi.org/10.1364/OE.521239.

[20] A. Annunziato, F. Anelli, A.M. Loconsole, V.V. Francione, S. Cozic, S. Venck, S. Poulain, F. Prudenzano, Single-mode fluoroindate coupler for mid-IR applications, in: S. Taccheo, M.R. Cicconi, M.L. Jäger (Eds.), Fiber Lasers and Glass Photonics: Materials through Applications IV, SPIE, 2024, p. 29, https://doi.org/10.1117/12.3017514.

[21] J. Meyer, W. Bewley, C. Canedy, C. Kim, M. Kim, C. Merritt, I. Vurgaftman, The Interband Cascade Laser, Photonics 7 (2020) 75, https://doi.org/10.3390/photonics7030075.

[22] F. Alimagham, M. Platkov, J. Prestage, S. Basov, G. Izakson, A. Katzir, S.R. Elliott, T. Hutter, Mid-IR evanescent-field fiber sensor with enhanced sensitivity for volatile organic compounds, RSC Adv. 9 (2019) 21186–21191, https://doi.org/10.1039/C9RA04104D.

[23] D. Noordegraaf, M.D. Maack, P.M.W. Skovgaard, J. Johansen, F. Becker, S. Belke, M. Blomqvist, J. Laegsgaard, All-fiber 7x1 signal combiner for incoherent laser beam combining, in: J.W. Dawson (Ed.), Fiber Lasers VIII: Technology, Systems, and Applications, SPIE, 2011, p. 79142L, https://doi.org/10.1117/12.875078.

[24] Y. Jaouen, L. du Mouza, D. Barbier, J.-M. Delavaux, P. Bruno, Eight-wavelength Er-Yb doped amplifier: combiner/splitter planar integrated module, IEEE Photonics Technol. Lett. 11 (1999) 1105–1107, https://doi.org/10.1109/68.784202.

[25] K. Kinjalk, F. Paciolla, B. Sun, A. Zifarelli, G. Menduni, M. Giglio, H. Wu, L. Dong, D. Ayache, D. Pinto, A. Vicet, A. Baranov, P. Patimisco, A. Sampaolo, V. Spagnolo, Highly selective and sensitive detection of volatile organic compounds using long wavelength InAs-based quantum cascade lasers through quartz-enhanced photoacoustic spectroscopy, Appl. Phys. Rev. 11 (2024), https://doi.org/10.1063/5.0189501.

[26] A.F.P. Cantatore, G. Menduni, A. Zifarelli, P. Patimisco, M. Gonzalez, H.R. Seren, V. Spagnolo, A. Sampaolo, Lithium niobate – enhanced photoacoustic spectroscopy, Photoacoustics 35 (2024) 100577, https://doi.org/10.1016/j.pacs.2023.100577.

[27] P. Patimisco, G. Scamarcio, F. Tittel, V. Spagnolo, Quartz-enhanced photoacoustic spectroscopy: a review, Sensors 14 (2014) 6165–6206, https://doi.org/10.3390/s140406165.

[28] Y. Liu, S. Qiao, C. Fang, Y. He, H. Sun, J. Liu, Y. Ma, A highly sensitive LITES sensor based on a multi-pass cell with dense spot pattern and a novel quartz tuning fork with low frequency, 230230–230230, Opto-Electron. Adv. 7 (2024), https://doi.org/10.29026/oea.2024.230230.
[29] C. Liu, G. Wang, C. Zhang, P. Patimisco, R. Cui, C. Feng, A. Sampaolo, V. Spagnolo, L. Dong, H. Wu, End-to-end methane gas detection algorithm based on transformer and multi-layer perceptron, Opt. Express 32 (2024) 987, https://doi.org/10.1364/OE.511813.
[30] S. Manohar, D. Razansky, Photoacoustics: a historical review, Adv. Opt. Photonics 8 (2016) 586, https://doi.org/10.1364/AOP.8.000586.
[31] T. Yang, W. Chen, P. Wang, A review of all-optical photoacoustic spectroscopy as a gas sensing method, Appl. Spectrosc. Rev. 56 (2021) 143–170, https://doi.org/10.1080/05704928.2020.1760875.
[32] S. Qiao, Y. He, H. Sun, P. Patimisco, A. Sampaolo, V. Spagnolo, Y. Ma, Ultra-highly sensitive dual gases detection based on photoacoustic spectroscopy by exploiting a long-wave, high-power, wide-tunable, single-longitudinal-mode solid-state laser, Light Sci. Appl. 13 (2024) 100, https://doi.org/10.1038/s41377-024-01459-5.
[33] H. Luo, Z. Yang, R. Zhuang, H. Lv, C. Wang, H. Lin, D. Zhang, W. Zhu, Y. Zhong, Y. Cao, K. Liu, R. Kan, Y. Pan, J. Yu, H. Zheng, Ppbv-level mid-infrared photoacoustic sensor for mouth alcohol test after consuming lychee fruits, Photoacoustics 33 (2023) 100559, https://doi.org/10.1016/j.pacs.2023.100559.
[34] P. Patimisco, A. Sampaolo, H. Zheng, L. Dong, F.K. Tittel, V. Spagnolo, Quartz–enhanced photoacoustic spectrophones exploiting custom tuning forks: a review, Adv. Phys. X 2 (2017) 169–187, https://doi.org/10.1080/23746149.2016.1271285.
[35] Y. Ma, S. Qiao, R. Wang, Y. He, C. Fang, T. Liang, A novel tapered quartz tuning fork-based laser spectroscopy sensing, Appl. Phys. Rev. 11 (2024), https://doi.org/10.1063/5.0214874.
[36] H. Sun, S. Qiao, Y. He, Y. Liu, Y. Ma, Highly sensitive CH 4, C 2H 2 and CO simultaneous measurement LITES sensor based on multi-pass cell with overlapped spots pattern and QTFs with low resonant frequency, Opt. Express 32 (2024) 28183, https://doi.org/10.1364/OE.531925.
[37] N. Mac Dowell, P.S. Fennell, N. Shah, G.C. Maitland, The role of CO2 capture and utilization in mitigating climate change, Nat. Clim. Chang 7 (2017) 243–249, https://doi.org/10.1038/nclimate3231.
[38] J.N. Sharma, A. Al-Omran, S.S. Parvathy, Role of nitric oxide in inflammatory diseases, Inflammopharmacology 15 (2007) 252–259, https://doi.org/10.1007/s10787-007-0013-x.
[39] I.E. Gordon, L.S. Rothman, R.J. Hargreaves, R. Hashemi, E.V. Karlovets, F. M. Skinner, E.K. Conway, C. Hill, R.V. Kochanov, Y. Tan, P. Wcisło, A.A. Finenko, K. Nelson, P.F. Bernath, M. Birk, V. Boudon, A. Campargue, K.V. Chance, A. Coustenis, B.J. Drouin, J. –M. Flaud, R.R. Gamache, J.T. Hodges, D. Jacquemart, E.J. Mlawer, A.V. Nikitin, V.I. Perevalov, M. Rotger, J. Tennyson, G.C. Toon, H. Tran, V.G. Tyuterev, E.M. Adkins, A. Baker, A. Barbe, E. Canè, A.G. Császár, A. Dudaryonok, O. Egorov, A.J. Fleisher, H. Fleurbaey, A. Foltynowicz, T. Furtenbacher, J.J. Harrison, J. –M. Hartmann, V. –M. Horneman, X. Huang, T. Karman, J. Karns, S. Kassi, I. Kleiner, V. Kofman, F. Kwabia–Tchana, N. N. Lavrentieva, T.J. Lee, D.A. Long, A.A. Lukashevskaya, O.M. Lyulin, V. Yu Makhnev, W. Matt, S.T. Massie, M. Melosso, S.N. Mikhailenko, D. Mondelain, H. S.P. Müller, O.V. Naumenko, A. Perrin, O.L. Polyansky, E. Raddaoui, P.L. Raston, Z. D. Reed, M. Rey, C. Richard, R. Tóbiás, I. Sadiek, D.W. Schwenke, E. Starikova, K. Sung, F. Tamassia, S.A. Tashkun, J. Vander Auwera, I.A. Vasilenko, A.A. Vigasin, G.L. Villanueva, B. Vispoel, G. Wagner, A. Yachmenev, S.N. Yurchenko, The HITRAN2020 molecular spectroscopic database, J. Quant. Spectrosc. Radiat. Transf. 277 (2022) 107949, https://doi.org/10.1016/j.jqsrt.2021.107949.
[40] PAF2-4E - FiberPort, FC/PC & FC/APC, f= 4.0 mm, 2.0 - 5.0 μm, Ø1.17 mm Waist, (n.d.). ⟨https://www.thorlabs.com/thorproduct.cfm?partnumber=PAF2-4E⟩ (accessed October 31, 2024).
[41] ADM01 - Acoustic Detection Module for QEPAS, Hylok Fittings, BaF2 Windows, (n.d.). ⟨https://www.thorlabs.com/thorproduct.cfm?partnumber=ADM01⟩ (accessed October 31, 2024).
[42] P. Patimisco, A. Sampaolo, M. Giglio, S. dello Russo, V. Mackowiak, H. Rossmadl, A. Cable, F.K. Tittel, V. Spagnolo, Tuning forks with optimized geometries for quartz-enhanced photoacoustic spectroscopy, Opt. Express 27 (2019) 1401, https://doi.org/10.1364/OE.27.001401.
[43] F. Anelli, A. Annunziato, A.M. Loconsole, S. Venck, S. Cozic, F. Prudenzano, Mode-group selective photonic lantern based on indium fluoride optical fibers for mid-infrared, J. Light. Technol. (2024) 1–8, https://doi.org/10.1109/JLT.2024.3450115.
[44] M. Rezaei, G.T. Zeweldi, M.H.M. Shamim, M. Rochette, Single-mode optical fiber couplers made of fluoride glass, Opt. Express 31 (2023) 27183, https://doi.org/10.1364/OE.495464.
[45] D. Stachowiak, High-power passive fiber components for all-fiber lasers and amplifiers application—design and fabrication, Photonics 5 (2018) 38, https://doi.org/10.3390/photonics5040038.
[46] É . Ducharme, S. Virally, R.I. Becerra-Deana, C. Boudoux, N. Godbout, Viscosity of fluoride glass fibers for fused component fabrication, Appl. Opt. 61 (2022) 5031, https://doi.org/10.1364/AO.455528.
[47] J.J. Davenport, M. Diab, P.J. Deka, A. Tripathi, K. Madhav, M.M. Roth, Photonic lanterns: a practical guide to filament tapering, Opt. Mater. Express 11 (2021) 2639, https://doi.org/10.1364/OME.427903.
[48] Chalcogenide MWIR Fused Fiber Combiner, (n.d.). ⟨https://irflex.com/products/chalcogenide-mwir/⟩ (accessed January 9, 2025).
[49] E. X Berry, Human CO2 emissions have little effect on atmospheric CO2, Int. J. Atmos. Ocean. Sci. 3 (2019) 13, https://doi.org/10.11648/j.ijaos.20190301.13.
[50] A. Zifarelli, A.F.P. Cantatore, A. Sampaolo, M. Mueller, T. Rueck, C. Hoelzl, H. Rossmadl, P. Patimisco, V. Spagnolo, Multivariate analysis and digital twin modelling: alternative approaches to evaluate molecular relaxation in photoacoustic spectroscopy, Photoacoustics 33 (2023) 100564, https://doi.org/10.1016/j.pacs.2023.100564.
[51] M. Giglio, P. Patimisco, A. Sampaolo, G. Scamarcio, F.K. Tittel, V. Spagnolo, Allan deviation plot as a tool for quartz-enhanced photoacoustic sensors noise analysis, IEEE Trans. Ultrason Ferroelectr. Freq. Control 63 (2016) 555–560, https://doi.org/10.1109/TUFFC.2015.2495013.
[52] A.A. Kosterev, F.K. Tittel, D.V. Serebryakov, A.L. Malinovsky, I.V. Morozov, Applications of quartz tuning forks in spectroscopic gas sensing, Rev. Sci. Instrum. 76 (2005), https://doi.org/10.1063/1.1884196.
[53] L. Dong, A.A. Kosterev, D. Thomazy, F.K. Tittel, QEPAS spectrophones: design, optimization, and performance, Appl. Phys. B 100 (2010) 627–635, https://doi.org/10.1007/s00340-010-4072-0.

Luigi Melchiorre received his Bachelor's Degree in Electronic and Telecommunications Engineering in 2019 and his Master's Degree in Telecommunications Engineering in 2022 from the Polytechnic of Bari (Bari, Italy). Currently, he is pursuing a PhD in Industry 4.0 at the same institution. The aim of his PhD research activities is to design, characterize, and implement innovative optical trace gas sensors by means of photonic integration and non-linear optics, exploiting the Quartz-Enhanced Photo-Acoustic Spectroscopy (QEPAS) and the Light-Induced Thermo-Elastic Spectroscopy (LITES) techniques targeting applications in the industrial, environmental, chemical, and medical fields.

Francesco Anelli received the M.Sc. degree in 2021 in Electronic Engineering (cum laude) from the Politecnico di Bari, Bari, Italy, where he is currently working toward the Ph.D. degree in Electrical and Information Engineering. His research interests include the design, and the characterization of silica optical fiber grating sensors based on novel geometries for curvature, strain, and temperature monitoring; fluoride and chalcogenide fused optical fiber components such as couplers, combiners, and sensors for mid-infrared applications.

Giansergio Menduni received the M. S. degree (cum laude) in 2017 and the Ph.D. degree in 2021 in Electronic Engineering from the Polytechnic University of Bari. Since 2022, he is an Assistant Professor in Applied Physics at the Physics Department of Polytechnic University of Bari. His research activity is focused on the development of gas sensors based on Quartz-Enhanced Photoacoustic Spectroscopy (QEPAS) and Light-Induced Thermoelastic Spectroscopy (LITES) on the signal conditioning of Quartz Tuning Forks transducers.

Andrea Annunziato received the Ph.D. degree in Aerospace Sciences and Engineering in 2024 from the Politecnico di Bari, Bari, Italy. His research interests include the design, and the characterization of silica optical fiber grating sensors based on planar substrate and flat fiber for curvature, strain, and temperature detection, also in reinforced polymer materials; fluoride and chalcogenide fused optical fiber components such as couplers and combiners for all-in-fiber amplifiers and lasers in the mid-infrared spectral range.

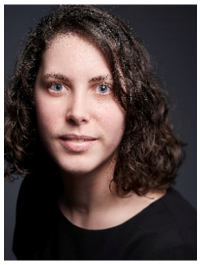

Laurine Bodin obtained the degree of engineer in photonics engineering from ENSSAT of Lannion (France) in 2016. Since 2015, she is employed at Le Verre Fluoré in the fiber qualification and integration department. Her activities are focused on the management of the standard fiber patch cable production line and the development of custom fiber patch cables, laser modules and fiber bundles. She is also responsible of all astronomical projects assembly and had worked on the SPIP project in 2020.

Solenn Cozic is Chief Operations Officer and Chief Scientist at Le Verre Fluoré. She obtained her PhD in material science in 2016 at Rennes University (France). Her PhD thesis focused on chalcogenide glasses: their electrical and structural properties for energy storage. She joined Le Verre Fluoré 8 years ago, specializing in fluoride glasses and optical fibers. She works on fluoride glass properties, novel fiber designs and fiber component development for UV, visible and mid-infrared applications.

Giovanni Magno obtained his PhD in Electronic Engineering from the Polytechnic University of Bari in 2015. From 2015 to 2020, he worked as a researcher at the C2N-CNRS in Palaiseau, France. His research focused on advanced nanoscience projects, including design and characterization of integrated plasmonic tweezers for particle manipulation, plasmonic nanoantennas, and development of opto-thermal simulators for analyzing laser-matter interactions in manufacturing processes. Since December 2020, he has been an Assistant Professor of Electromagnetic Fields at the Electrical and Information Engineering Department of the Polytechnic University of Bari. Currently, his research activity centers on designing and characterizing optical and microwave devices, with a particular emphasis on optical metasurfaces for augmented reality and reconfigurable reflective intelligent surfaces utilizing graphene.

Angelo Sampaolo obtained his Master degree in Physics in 2013 and the PhD Degree in Physics in 2017 from University of Bari. He was an associate researcher in the Laser Science Group at Rice University from 2014 to 2016 and associate researcher at Shanxi University since 2018. Since 2019, he is Assistant Professor at Polytechnic of Bari. His research activity has focused on the development of innovative techniques in trace gas sensing, based on Quartz-Enhanced Photoacoustic Spec troscopy and covering the full spectral range from near-IR to THz.

Francesco Prudenzano received the Ph.D. degree in electronic engineering from the Politecnico di Bari, Bari, Italy, in November 1996. Since 2018, he has been a Full Professor of electromagnetic fields with the Department of Electrical and Information Engineering, Politecnico di Bari. His research interests include the design and characterization of microwave devices, integrated optics, and optical fiber-based devices. He is the Head of Microwave and Optical Engineering Group, Department of Electrical and Information Engineering, Politecnico di Bari. From 2017 to 2018, he was the Chair of SIOF, Italian Society of Optics and Photonics (Italian branch of EOS - European Optical Society). He has coauthored more than 400 publications, 295 of which got published in journals and international conferences, lectures, and invited papers. He is involved in several national and international research projects and cooperations.

Vincenzo Spagnolo received the degree (summa cum laude) and the PhD, both in physics, from University of Bari. He works as Full Professor of Applied Physics at the Technical University of Bari. In 2019, he become Vice-Rector of the Technical Uni versity of Bari, deputy to Technology Transfer. Since 2017, he is the director of the joint-research lab PolySense, created by THORLABS GmbH and Technical University of Bari, devoted to the development and implementation of novel gas sensing techniques and the realization of highly sensitive QEPAS trace-gas sensors.